

Article

The Choice of the Optimal Number of Discs in an MR Clutch from the Viewpoint of Different Criteria and Constraints

Krzysztof Kluszczyński [†], Zbigniew Pilch ^{*,†}

Faculty of Electrical and Computer Engineering, Cracow University of Technology, Warszawska Str. 24, 31155 Cracow, Poland; krzysztof.kluszczyński@pk.edu.pl

* Correspondence: zbigniew.pilch@pk.edu.pl

† These authors contributed equally to this work.

Abstract: This paper focuses on magnetorheological clutches (MR clutches) with a disc structure that can be designed as one-disc or multi-disc clutches (number of discs: $N = 1, N > 2$). The main goal of the paper is to compare their overall dimensions (lengths and radii), masses, volumes, and characteristic factors—torque per mass ratio and torque per volume ratio for MR clutches that develop the same given clutching torque T_c but differ in the number of discs (it is assumed that the number of discs of the primary member varies from one to four). This analysis develops charts and guidelines that will allow designers to choose the appropriate number of discs from the view point of various criteria, and with various limitations regarding geometry, geometric proportions, mass, volume, or restrictions on the amount of active materials used in the manufacturing process. The limitations on the active materials used are of particular importance in the case of mass production. Our methodology uses a comparative study, which can also be used when comparing design solutions of other electromechanical converters.



Citation: Kluszczyński K.; Pilch Z. The Choice of the Optimal Number of Discs in an MR Clutch from the Viewpoint of Different Criteria and Constraints. *Energies* **2021**, *14*, 6888. <https://doi.org/10.3390/en14216888>

Academic Editors: Ryszard Palka and Marcin Wardach

Received: 25 August 2021
Accepted: 13 October 2021
Published: 20 October 2021

Publisher's Note: MDPI stays neutral with regard to jurisdictional claims in published maps and institutional affiliations.



Copyright: © 2021 by the authors. Licensee MDPI, Basel, Switzerland. This article is an open access article distributed under the terms and conditions of the Creative Commons Attribution (CC BY) license (<https://creativecommons.org/licenses/by/4.0/>).

Keywords: electromechanical converter; drive system component; electromagnetic calculation; MR fluids; MR multi-disc clutch; clutch design

1. Introduction

Magnetorheological (MR) fluids belong to the group of Smart Materials [1–3]. The feature of MR fluids that can be controlled with the help of an external magnetic field (generated by an excitation winding) is viscosity: the stronger the magnetic field, the greater the viscosity. Because of this property, MR fluids have found a number of applications in dampers [4] and brakes [1,5,6]. MR clutches are a very promising application, in which the coupling between two mechanical parts is brought about through magnetic means and not by mechanical contact. The structure of MR clutches can be divided into two basic varieties: a cylindrical structure or a disc type [7,8]. The latter can include one disc of the primary member (number of discs $N = 1$), or many discs (multi-disc construction with $N \geq 2$) [9]. This paper focuses on a multi-disc MR clutch. The many possibilities of varying the geometrical proportions of MR clutches by selecting different numbers of discs appears to be a key advantage. They play a particularly important role in embedded drive systems applied in the automotive [10–13], aerospace, shipbuilding and robotics industries [14].

An example of a three-disc MR clutch is given in Figures 1 and 2: the main view with the description of consecutive constructional parts is presented in Figure 1 and an axis-symmetrical cross-section (due to symmetry, it is sufficient to consider only half of the cross-section) is presented in Figure 2.

The coil wound on a carcass is presented separately in Figure 3. It consists of z turns. The diameter of a bare conductor is denoted by d_{Cu} and the diameter of an insulated conductor by d_{Cu0} .

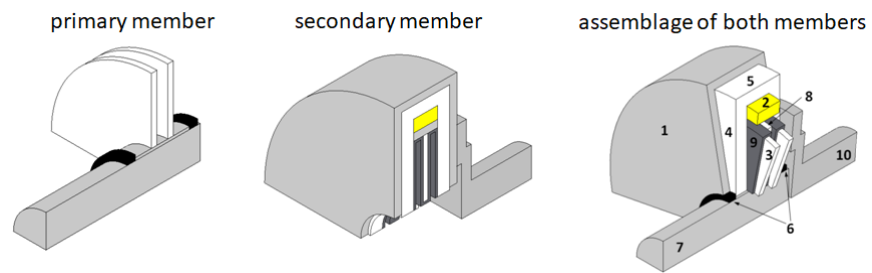


Figure 1. Main view of a two-disc ($N = 2$) MR clutch: 1—non-magnetic housing, 2—coil, 3—discs of primary member, 4—cover yoke, 5—cylinder yoke, 6—bearings, 7—non-magnetic shaft—primary member, 8—discs of secondary member, 9—MR fluid, 10—non-magnetic shaft—secondary member.

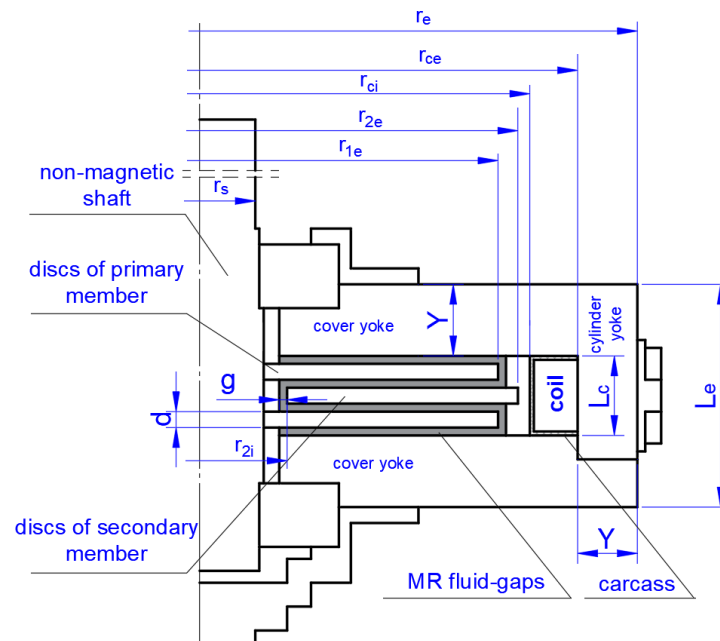


Figure 2. Axisymmetrical cross-section of a two-disc MR clutch ($N = 2$): L_e —external length of magnetic circuit, r_e —external radius of magnetic circuit, r_s —radius of non-magnetic shaft, r_{1e} —external radius of primary member discs, r_{2e} —external radius of secondary member discs, r_{2i} —inner radius of secondary member discs, d —thickness of primary and secondary member discs, g —thickness of MR fluid gap, L_c —external length of coil, r_{ce} —external radius of coil, r_{ci} —inner radius of coil, Y —thickness of cover and cylinder yoke.

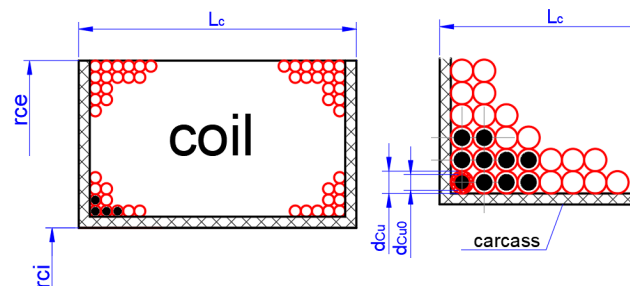


Figure 3. Dimensions of coil and conductors.

The value of the excitation current I feeding the coil is usually given; its value results from the properties of the supply system. The current density in the coil must be selected such that a satisfactory efficiency can be obtained without an excessive temperature increase. Assuming that the allowable current density for the given insulation class of wound wires

is $j_{cu} = 4.5 \text{ A/mm}^2$, one can calculate the values of the cross-sectional area S_{cu} , and the diameter of a bare conductor d_{cu} .

$$S_{cu} = \frac{I}{j_{cu}}, \quad (1)$$

$$d_{cu} = \sqrt{\frac{4 \cdot S_{cu}}{\pi}}. \quad (2)$$

The final nominal cross-sections and diameters of the bare conductors S_{cu0} and d_{cu0} , and the insulated conductors S_{cu} and d_{cu} , that are used to wind the coil can be found in the AWG International Standard Specification [15].

Note that the terminology used for the description of the MR clutch in Figures 1–3 is inspired by that used in the theory of transformers and electrical machines.

2. Materials and Methods

2.1. Assumptions that Must Be Fulfilled by the Compared Clutches with the Number of Discs $N = 1, 2, 3, 4$

In the framework of a comparative study, we decided to compare clutches with a number of discs in the primary member varying from one to four ($N = 1, 2, 3, 4$) and developing a clutching torque equal to: $T_c = 20, 35, 50 \text{ Nm}$. The comparison was made under the following assumptions:

- The thickness of the MR fluid gap g is assumed the same ($g = 1 \text{ mm}$);
- Current density j_{Cu} is assumed the same (it is assumed that $j_{Cu} = 4.5 \text{ A/mm}^2$ Equations (1) and (2));
- Excitation current I is assumed the same ($I = 0.6 \text{ A}$);
- Allowable stress k_s is assumed the same $k_s = 75 \times 10^6 \text{ Pa}$. Usually the designer introduces an additional safety factor k_{safe} by which the given value of the clutching torque is multiplied to determine the shaft radius r_s ensuring the appropriate level of safety;
- Safety factor for shaft k_{safe} is assumed the same $k_{safe} = 1.2$;
- The B-H curve for magnetic steel forming a ferromagnetic core is depicted in Figure 4a and the B-H curve for MR fluid MRF-140CG is depicted in Figure 4b [16];
- It is assumed that discs and yokes are made of the same magnetic steel;
- Magnetic flux density in MR fluid-gaps B_0 is kept the same in spite of variations in the geometries of clutches (the recommended value resulting from [12,17] is equal to $B_0 = 0.7 \text{ T}$). More precisely, B_0 is the magnetic flux density in the middle of the MR fluid gap, and can be regarded as “its average value”;
- Maximum magnetic field density B_{mx} is kept the same in spite of variations in the geometries of clutches. The most saturated point lies within the cover yoke at a length approximately equal to the external radius of the primary member discs [18,19] (we assumed a value of $B_{mx} = 1.2 \text{ T}$ located at the knee of the B-H curve for magnetic steel, which is remarkably less than the saturation point 1.6 T);

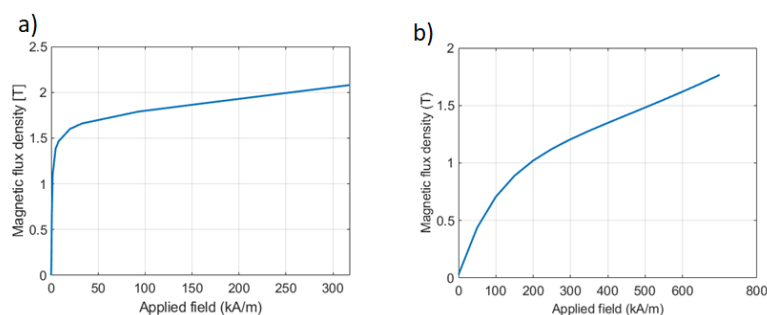


Figure 4. B-H curves for magnetic steel and MR fluid MRF-140CG. (a) B-H curves for ferromagnetic steel [20]. (b) B-H curves for MR fluid MRF-140CG [16].

2.2. Brief Description of the Applied Analytical-Field Design Method and Obtained Constructional Data for the Considered Variants

The design method that we used in the comparative study includes two stages: an analytical stage (composed of 36 algebraic formulas) and a field stage based on the finite element method (FEM). The analytical stage allows for a preliminary, quick determination of the approximate geometric dimensions and data of the excitation coil for the designed clutch, which develops the given torque T_c and meets all the assumptions listed in m. The final determination of the value of the clutching torque, the distribution of the magnetic field, the total magnetomotive force, the geometrical dimensions of the clutch and the data of the excitation coil are made in the field stage. From the point of view of the field stage, the analytical stage is a preliminary stage that allows us to determine a starting point close to the solution sought, which allows a significant reduction in the number of iterations and the computation time.

The clutching torque occurs in the space between the $2N$ overlapping surfaces of: N primary member discs, $N - 1$ secondary member discs and 2 internal surfaces of cover yokes facing the discs. In the analytical stage, the approximate value of the clutching torque is calculated according to the following formula:

$$T_c = 2N \cdot \int_{r_{2i}}^{r_{1e}} \int_0^{2\pi} dT = 2N \cdot \int_{r_{2i}}^{r_{1e}} \int_0^{2\pi} \tau_y(B_0) \cdot r^2 \cdot d\phi dr = \frac{4\pi}{3} \cdot N \cdot \tau_y(B_0) \cdot (r_{1e}^3 - r_{2i}^3), \tag{3}$$

where, $\tau_y(B)$ is a shear stress vs. magnetic flux density B curve, resulting from the Bingham model for plastics depicted in Figure 5 (in a clutch functioning in shear mode, the primary and secondary member discs do not move relative to each other, so $\dot{\gamma} = 0$). As seen, for the assumed value of magnetic flux density in the MR fluid-gaps $B_0 = 0.7$ T, shear stress is equal to: $\tau_y(B_0 = 0.7 \text{ T}) = 45.7$ kPa (Figure 5b).

In the field stage, the exact value of clutching torque is determined on the basis of the real spatial distribution of magnetic flux density resulting from the FEM model, according to the following formula (Figure 6):

$$T_c = \sum_{i=1}^{2N} T_{ci} = \sum_{i=1}^{2N} \int_{r_{2i}}^{r_{1e}} \int_0^{2\pi} \tau_y[B_i(r, \phi)] dr d\phi, \tag{4}$$

where i is the number of the considered surface, r is the current radius, $d\phi$ is the angle increment and dr is the radius increment.

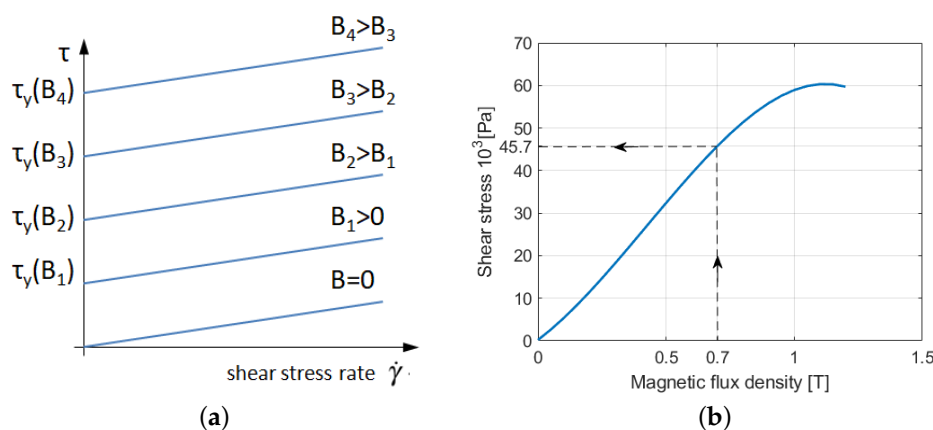


Figure 5. Graphical representation of Bingham model (a). Yield stress characteristics $\tau(B)$ for MRF-140CG [16] (b).

The FEM model is based on an open-access program Agros2D that was elaborated at the Pilzen University of Technology [20] (all of the scripts were written in PythonLAB language).

In the elaborated analytical-field method, the crucial role is played by the so-called yoke factor k_Y , the concept of which is based on the theory of induction machines. To define

the yoke factor, it is necessary to introduce the term of the movement region. The movement region consists of the overlapping fragments of N primary member discs, $N - 1$ secondary member discs, $2N$ MR fluid-gaps and 2 internal surfaces of cover yokes facing the discs. The exact boundaries of the movement region on the example of a magnetorheological clutch with 2 primary member discs (2-disc MR clutch) are shown in Figure 7.

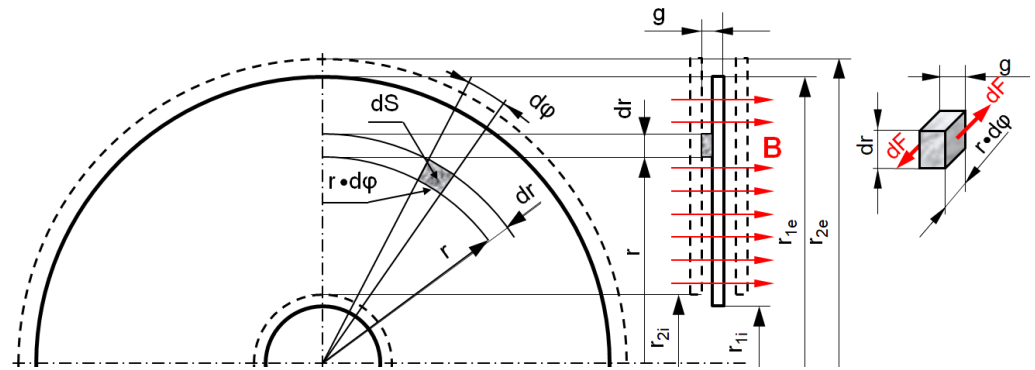


Figure 6. Geometrical denotations for calculating clutching torque acting on a single disc surface.

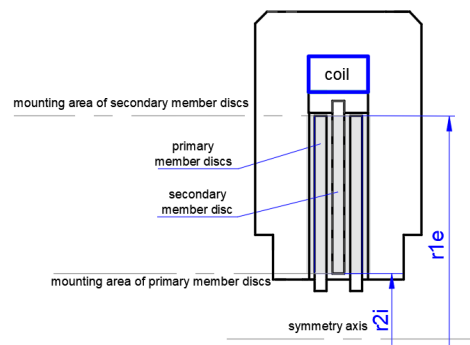


Figure 7. Exact boundaries of the movement region in the example of a magnetorheological clutch with 2 primary member discs (2-disc MR clutch).

The yoke factor determines the ratio of the total magnetomotive force required to magnetise the entire magnetic circuit of the clutch, $\Theta = \Theta_{mr} + \Theta_Y$ (where: Θ —the total magnetomotive force, Θ_{mr} —the magnetomotive force required to magnetise the movement region, Θ_Y —the magnetomotive force required to magnetise the yoke region composed of two covers and a cylinder) to the magnetomotive force Θ_{mr} :

$$k_Y = \frac{\Theta}{\Theta_{mr}} = \frac{\Theta_{mr} + \Theta_Y}{\Theta_{mr}}. \tag{5}$$

In the analytical stage, the approximate value of the total magnetomotive force is calculated according to the following formula:

$$\Theta = k_Y \cdot \Theta_{mr} = k_Y \cdot \left[\underbrace{2Ng \cdot \frac{B_0}{\mu_0 \mu_{MR}(B_0)}}_{\Theta_{mr(MR)}} + \underbrace{(2N - 1)d \cdot \frac{B_0}{\mu_0 \mu_{Fe}(B_0)}}_{\Theta_{mr(Fe)}} \right], \tag{6}$$

where $\Theta_{mr(MR)}$ is the magnetomotive force associated with the MR fluid gaps, $\Theta_{mr(Fe)}$ is the magnetomotive force associated with the discs, $\mu_{MR}(B_0)$ is determined from the curve in Figure 4b, and $\mu_{Fe}(B_0)$ is determined from the curve in Figure 4a.

In the field stage, the exact value of the total magnetomotive force is determined on the basis of the real spatial distribution of magnetic flux density and the real value of the yoke factor k_Y determined using loop calculations. As shown in Figure 8, the applied

analytical field-design method works according to the block diagram with iteration loop factor k_Y .

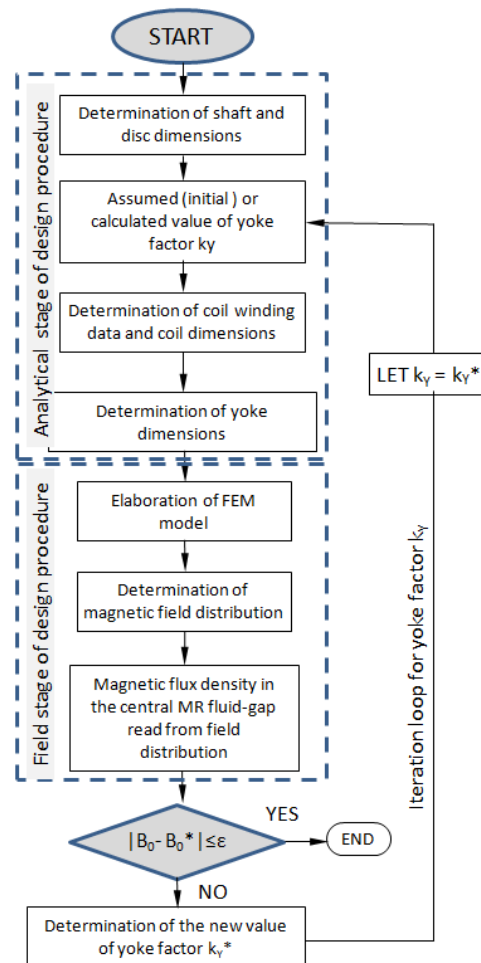


Figure 8. The applied analytical field-design method: block diagram.

The results of design calculations: magnetic field distributions and constructional data for the selected variants with the greatest considered values and the lowest considered values of the clutching torque and the number of discs:

- variant 1: $T_c = 20 \text{ Nm}$, $N = 1$ (Figure 9a);
- variant 2: $T_c = 20 \text{ Nm}$, $N = 4$ (Figure 9b);
- variant 3: $T_c = 50 \text{ Nm}$, $N = 1$ (Figure 9c);
- variant 4: $T_c = 50 \text{ Nm}$, $N = 4$ (Figure 9d);

are given in Figure 9 and in Table 1, respectively. In Figure 10 these variants are located in the corners of the table and are marked by green line contours.

Table 1 shows how the geometrical (constructional) parameters specified in Figure 2, as well as the total magnetomotive force Θ , the number of coil turns z and the yoke factor k_Y change for the four selected clutches with a different number of discs and different ratings, while maintaining the assumptions listed in Section 2.1.

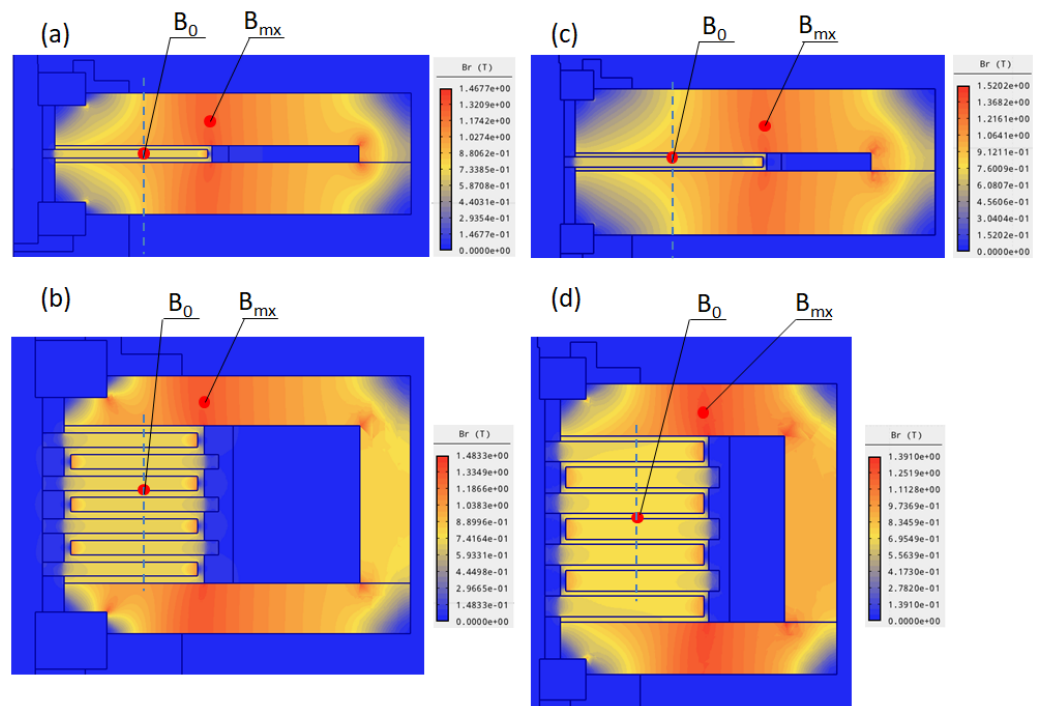


Figure 9. Magnetic field distribution for the selected variants: variant 1 (a), variant 2 (b), variant 3 (c), variant 4 (d).

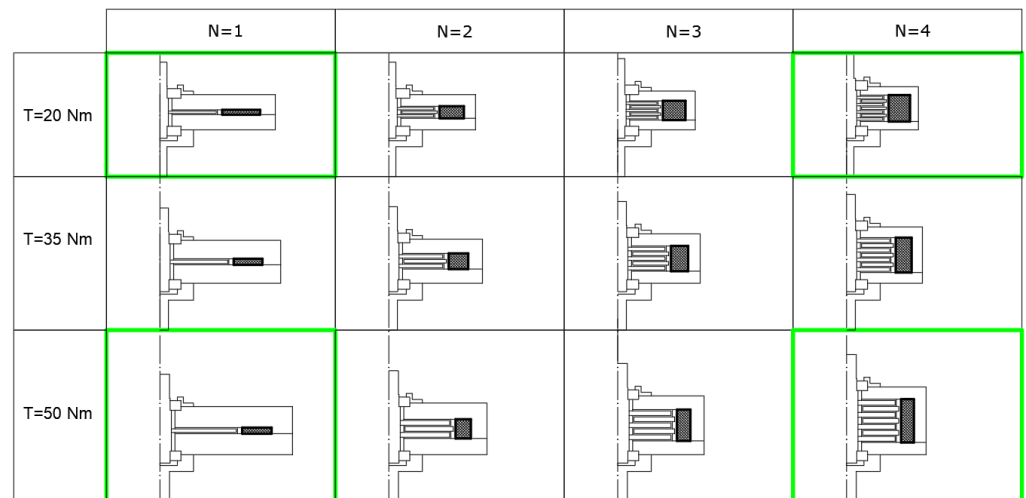


Figure 10. Graphical overview of cross-sections for the 12 designed variants: $T_c = 20 \text{ Nm}$, $N = 1,2,3,4$, $T_c = 35 \text{ Nm}$, $N = 1,2,3,4$ and $T_c = 50 \text{ Nm}$, $N = 1,2,3,4$.

For a comparative study, which is the main goal and essence of the paper, we use our own analytical-field design method—the idea of which, was briefly described in this chapter. This method was verified experimentally on the example of the constructed 5-disc MR clutch presented in [21]. The detailed step-by-step description of this integrated method is presented in [22]. Someone who wishes to replicate the comparative study can also use his own design method (field, analytical or field-analytical) and his own method for choosing the most favourable starting point.

Table 1. The results of the design calculations for the selected variants.

| | | var. 1 | var. 2 | var. 3 | var. 4 |
|---|---------------|--------|--------|--------|--------|
| radius of shaft | r_s (mm) | 5.9 | 6.1 | 8 | 8.1 |
| thickness of discs | d (mm) | 2 | 2 | 3 | 4 |
| thickness of MR fluid gap | g (mm) | 1 | 1 | 1 | 1 |
| inner radius of secondary member discs | r_{2i} (mm) | 11 | 12.5 | 13.5 | 13.5 |
| external radius of primary member discs | r_{1e} (mm) | 47 | 30.2 | 63.7 | 40.5 |
| external radius of secondary member discs | r_{2e} (mm) | 50 | 33.2 | 66.7 | 43.5 |
| inner radius of coil | r_{ci} (mm) | 52 | 35.2 | 68.7 | 45.5 |
| external radius of coil | r_{ce} (mm) | 83.5 | 52.9 | 93.1 | 56.1 |
| external length of coil | L_c (mm) | 4 | 22 | 5 | 36 |
| thickness of cover and cylinder yoke | Y (mm) | 12.7 | 7 | 17.5 | 10.2 |
| number of coil turns | z (-) | 364 | 1364 | 367 | 1363 |
| yoke factor | k_Y (-) | 1.259 | 1.176 | 1.270 | 1.176 |
| total magnetomotive force | Θ (A) | 173.6 | 347.3 | 520.9 | 694.5 |
| external radius of magnetic circuit | r_e (mm) | 96.2 | 59.9 | 110.6 | 66.3 |
| external length of magnetic circuit | L_e (mm) | 29.4 | 36 | 40 | 56.4 |

3. Results

3.1. Results of Comparative Study for the MR Clutches $T_c = 20, 35, 50$ Nm with Number of Discs $N = 1, 2, 3, 4$

A comparative analysis of the external (overall) dimensions, masses and volumes, as well as the characteristic coefficients relating to the use of active materials and the space occupied, was carried out for MR clutches developing a clutching torque $T_c = 20, 35, 50$ Nm with the number of primary member discs varying from $N = 1$ to $N = 4$. A group of charts referring to total lengths L , external radius r_e , their masses m and volumes V [6], as well as the coefficients: T_c/m ratio and T_c/V ratio are presented in Figures 11a,b, 12a,b and 13a,b, respectively.

To select the correct number of discs, different aspects must be considered, the most important of which is the limitations imposed either on the outer dimensions or on the mass and volume specified by the user, based on the planned or expected applications, e.g., in automotive/motorcycle drive systems or disengagement auxiliaries in automotive/aviation/ship industries.

In the electromechanical industry, the values of torque per mass and torque per volume play an important role when comparing various possible solutions. The greater the developed torque, for the same mass or volume of an electric machine or electromagnetic device, the better the obtained solution is at utilising the full use of construction materials (or a better use of space occupied by the machine or device).

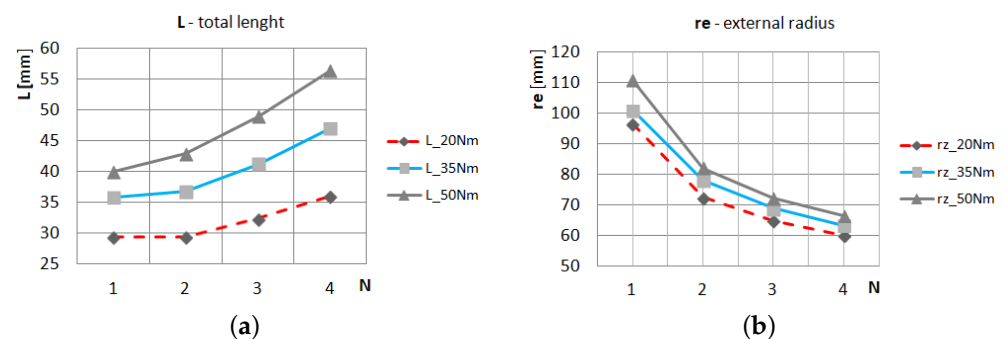


Figure 11. Total length vs. number of discs N (a) and external radius vs. number of discs N (b) for MR clutches $T_c = 20, 35, 50$ Nm.

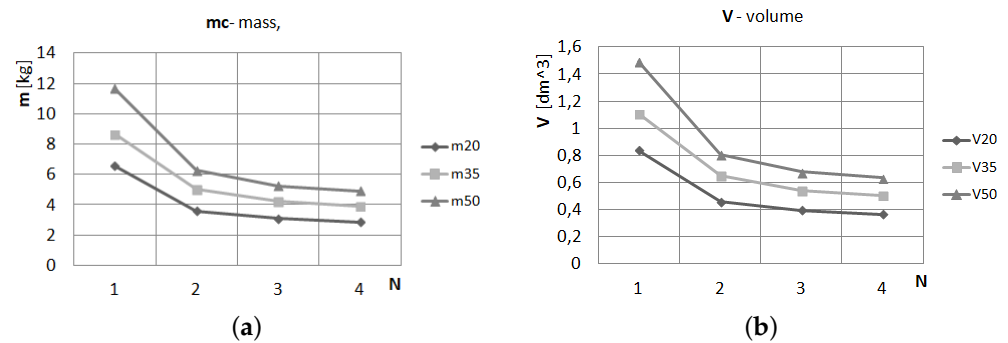


Figure 12. Mass vs. number of discs N (a) and volume vs. number of discs N (b) for MR clutches $T_c = 20, 35, 50$ Nm.

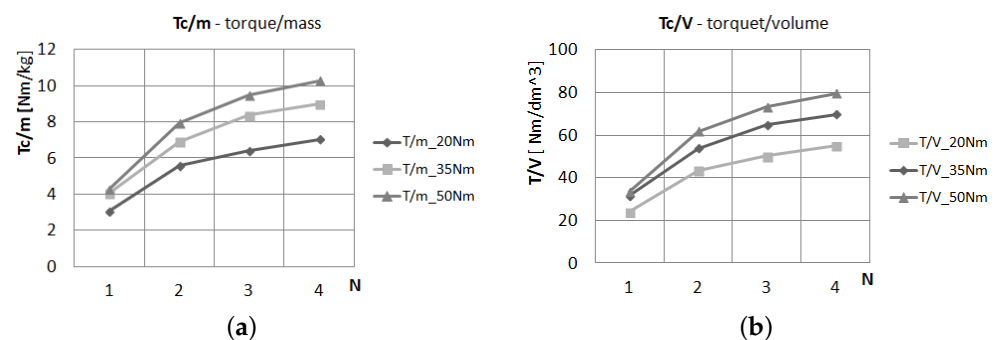


Figure 13. T_c/m ratio vs. number of discs N (a) and T_c/V ratio vs. number of discs N (b) for MR clutches $T_c = 20, 35, 50$ Nm.

As can be seen in Figure 11a, increasing the number of discs leads to an increase in the length of the clutch (an increase in length is more significant when the torque developed by the clutch is greater) and a decrease in the external radius of the clutch Figure 11b.

It should be noted that the clutches $T_c = 20$ Nm with $N = 1$ and $N = 2$ have the same total length L (Figure 11a), which results from the fact that the clutch with $N = 2$ has a much thinner cover. For the abovementioned clutches, the increase in length of the movement region is compensated for by a decrease in the thickness of the yoke covers: $Y_{N=1} = 12.7$ mm, $Y_{N=2} = 9.7$ mm. For the clutches $T_c = 20$ Nm with $N = 3$ and $N = 4$, the increase in total length L (in relation to the length of clutch $N = 1$) is 10% and 22.5%, respectively, while the decrease in the cover thickness is less pronounced $Y_{N=3} = 8.2$ mm, $Y_{N=4} = 7$ mm.

As seen in Figure 12a,b, the increase in the number of discs leads to a distinctly visible reduction in the masses and volumes of the MR clutches. The selected number of discs is typically a compromise between the mass or volume of the clutch, which decreases with the number of discs and the technological complexity or production costs that increase with the number of discs. As seen in Figure 12, an asymptotic trend of the charts occurs, which means that it does not make sense to consider variants with $N > 4$ discs, due to the rapidly increasing complexity of the design, as well as increasing manufacturing costs.

Regarding the ratios: T_c/m and T_c/V (Figure 13a,b), a clearly visible increase in their value is noticeable when changing the number of discs from $N = 1$ to $N = 2$. The course of the charts for clutches with $N > 2$ also becomes increasingly flat. From the point of view of the above ratios, the recommended number of primary discs is $N = 2$.

The graphs shown in Figures 11a,b or 12a,b are useful for determining the number of discs where total length L , external radius r_e , mass m or volume V are limited. Graphical overview of cross-sections for the 12 designed variants: $T_c = 20$ Nm, $N = 1, 2, 3, 4$, $T_c = 35$ Nm, $N = 1, 2, 3, 4$ and $T_c = 50$ Nm, $N = 1, 2, 3, 4$ are given in Figure 10.

3.2. Detailed Analysis of the Case: $T_c = 20 \text{ Nm}$ and Physical Explanation of the Obtained Results

This chapter is devoted to a detailed analysis of the impact of the number of primary member discs ($N = 1, 2, 3, 4$) on selected design data on the example of an MR clutch developing torque $T_c = 20 \text{ Nm}$.

The consecutive Figures 14–16 show total lengths L (Figure 14) and radii r_e , masses m and volumes V (Figure 15), ratios T_c/m and T_c/V (Figure 16) together in a combined figure, which makes it possible to evaluate the rate of change of important constructional design parameters when increasing the number of discs.

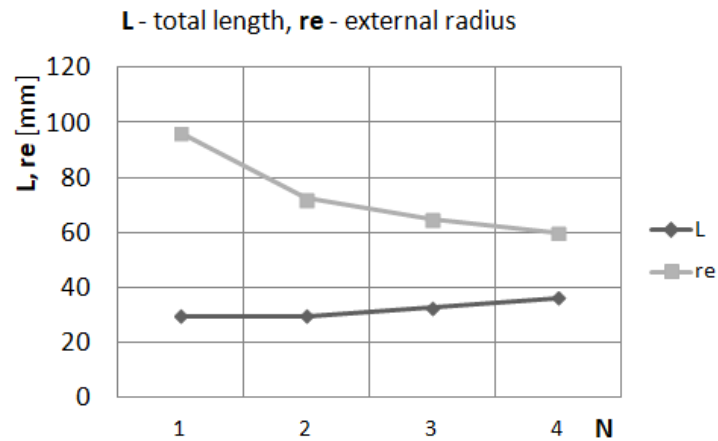


Figure 14. Total lengths L and external radius r_e vs. number of discs N .

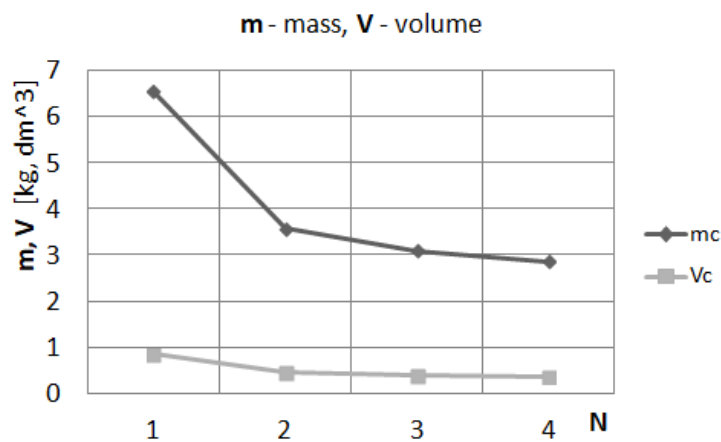


Figure 15. Mass m and volume V vs. number of discs N .

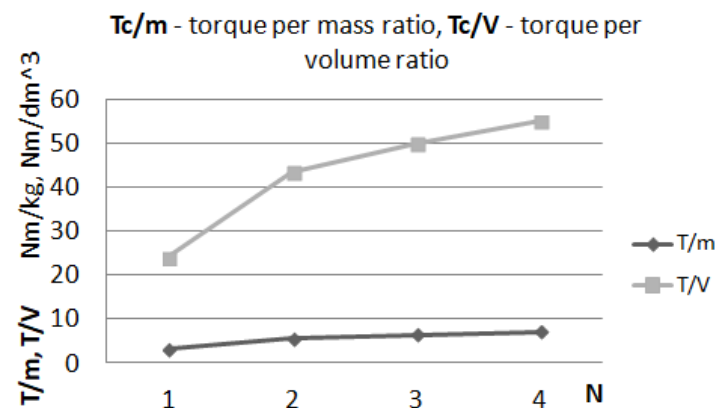


Figure 16. Torque per mass ratio T_c/m and torque per volume ratio T_c/V vs. number of discs N .

An important aspect that must be taken into account in the mass production of electrical machines and electromagnetic devices with magnetorheological (MR) fluid is the total mass of copper (Cu), the total mass of ferromagnetic steel (Fe) and the total mass of MR fluid, due to the constantly changing market prices of construction materials. The design that is accepted and approved for production is always a compromise between the best possible technical supplies (operating data) and the lowest production costs. The charts presented in Figure 17 will be important in reducing the total cost of the above-mentioned active materials (magnetic steel, copper and MR fluid) used in the mass production of clutches.

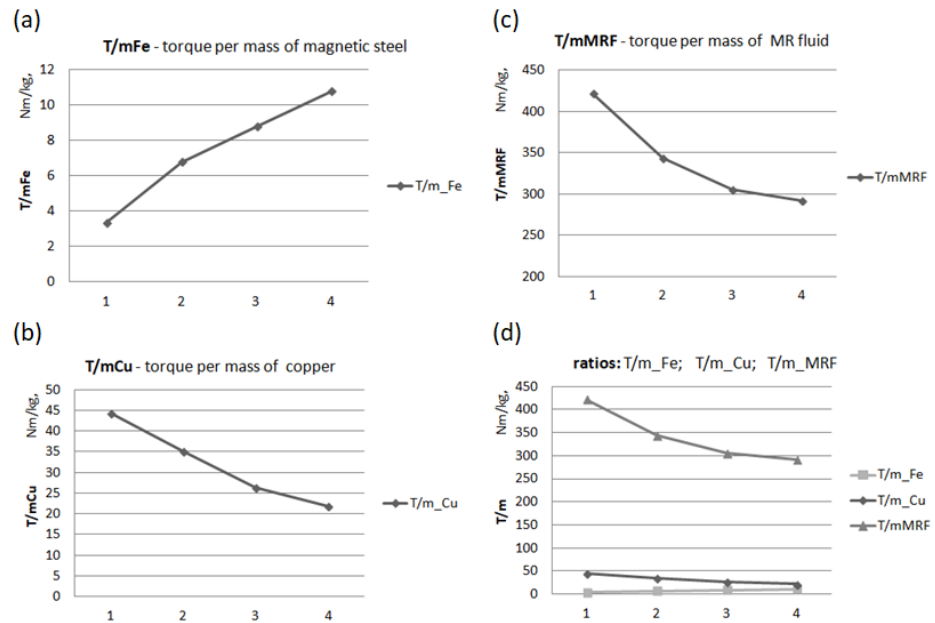


Figure 17. Torque per magnetic steel mass (a), torque per copper mass (b), torque per MR fluid mass (c) and the complete set of charts (d).

Looking at Figure 10, we can easily explain significant decreases in the clutch mass and significant increases in torque per magnetic steel mass (especially when considering the variant $N = 2$ in reference to variant $N = 1$). The reason for that is the remarkable drop in the thickness of cover and cylinder yokes (Figure 18).

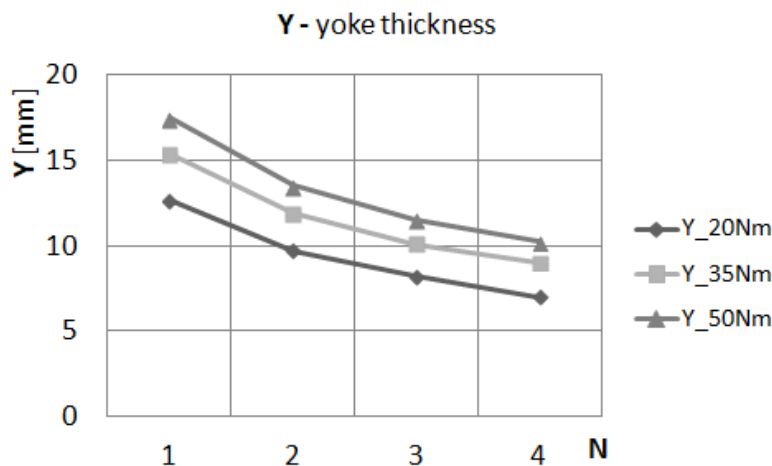


Figure 18. Yoke thickness vs. number of discs N for the clutch $T_c = 20$ Nm.

4. Discussion

This paper indicates the possibility of a different number of discs (from $N = 1$ to $N = 4$) in MR clutches and shows that each number of discs is associated with different properties, with respect to the overall dimensions, geometrical proportions, masses, volumes, clutching torque per mass ratio T_c/m and clutching torque per volume ratio T_c/V .

These numerous possibilities of varying the geometrical proportions of clutches and increasing the values of the abovementioned ratios by selecting different numbers of discs appears to be a particularly promising advantage. This is especially important in embedded drive systems applied in the automotive, aerospace, shipbuilding and robotics industries.

The results of this study are a set of charts and guidelines that allow designers to choose the appropriate number of discs from the viewpoint of various criteria and various constraints concerning the geometry, mass and costs of active materials.

Where there are no limitations regarding geometry and mass of a designed clutch or restrictions on the amount of active materials used in its manufacturing process, the optimal (recommended) number of discs is equal to $N = 2$.

In the case of devices with MR fluids, there is also the problem of possible degradation of the fluid properties during prolonged or improper use. Regarding the MR clutch, this may refer to excessively long running time of the clutch in case of slip. Determining the value of this unacceptable working time, and the value of the permissible slip, requires supplementing the developed clutch model with thermal calculations focused on the analysis of the temperature field distribution [23].

Author Contributions: Conceptualization, K.K. and Z.P.; methodology, K.K.; software, Z.P.; validation, Z.P., K.K.; formal analysis, Z.P., K.K.; writing—original draft preparation, Z.P.; writing—review and editing, Z.P.; visualization, Z.P.; supervision, K.K. All authors have read and agreed to the published version of the manuscript.

Funding: This research was conducted at the Faculty of Electrical and Computer Engineering, Cracow University of Technology.

Institutional Review Board Statement: Not applicable.

Informed Consent Statement: Not applicable.

Data Availability Statement: MDPI Research Data Policies.

Conflicts of Interest: The authors declare no conflict of interest. The funders had no role in the design of the study; in the collection, analyses, or interpretation of data; in the writing of the manuscript, or in the decision to publish the results.

Sample Availability: Samples of the compounds are available from the authors.

Abbreviations

The following abbreviations are used in this manuscript:

MR clutches Magnetorheological clutches

References

1. Chen, J.Z.; Liao, W.H. Design, testing and control of a magnetorheological actuator for assistive knee braces. *Smart Mater. Struct.* **2010**, *19*, 035029. [[CrossRef](#)]
2. Kciuk, M.; Chwastek, K.; Kluszczyński, K.; Szczygłowski, J. A study on hysteresis behaviour of SMA linear actuators based on unipolar sigmoid and hyperbolic tangent functions. *Sens. Actuators A Phys.* **2016**, *243*, 52–58. [[CrossRef](#)]
3. Kim, K.J.; Lee, C.W.; Koo, J.H. Design and modelling of semi-active squeeze film dampers using magneto-rheological fluids. *Smart Mater. Struct.* **2008**, *17*, 035006. [[CrossRef](#)]
4. Martynowicz, P. Study of Vibration Control Using Laboratory Test Rig of Wind Turbine Tower-Nacelle System with MR Damper Based Tuned Vibration Absorber. *Bull. Pol. Acad. Sci. Tech. Sci.* **2016**, *64*, 347–359. [[CrossRef](#)]
5. Rossa, C.; Jaegy, A.; Lozada, J.; Micaelli, A. Design Considerations for Magnetorheological Brakes. *Trans. Mechatronics* **2014**, *19*, 1669–1680. [[CrossRef](#)]

6. Nguyen, Q.H.; Choi, S.B. Selection of magnetorheological brake types via optimal design considering maximum torque and constrained volume. *Smart Mater. Struct.* **2011**, *21*, 015012. [CrossRef]
7. Li, W.H.; Du, H. Design and Experimental Evaluation of a Magnetorheological Brake. *Int. J. Adv. Manuf. Technol.* **2003**, *21*, 508–515. [CrossRef]
8. Rizzo, R.; Musolino, A.; Bucchi, F.; Forte, P.; Frenzo, F. Magnetic FEM Design and Experimental Validation of an Innovative Fail-Safe Magnetorheological Clutch Excited by Permanent Magnets. *IEEE Trans. Energy Convers.* **2014**, *29*, 628–640 [CrossRef]
9. Karakoc, K.; Park, E.J.; Suleman, A. Design considerations for an automotive magnetorheological brake. *Mechatronics* **2008**, *18*, 434–447. [CrossRef]
10. East, W.; Turcotte, J.; Plante, J.-S.; Julio, G. Experimental assessment of a linear actuator driven by magnetorheological clutches for automotive active suspensions. *J. Intell. Mater. Syst. Struct.* **2021**, *32*, 955–970. [CrossRef] [PubMed]
11. Park, E.J.; Falcao, L.; Suleman, A. Multidisciplinary design optimization of an automotive magnetorheological brake design. *Comput. Struct.* **2008**, *28*, 207–216. [CrossRef]
12. Sohn, J.W.; Jeon, J.; Nguyen, Q.H.; Seung-Bok, C. Optimal design of disc-type magneto-rheological brake for mid-sized motorcycle: Experimental evaluation. *Smart Mater. Struct.* **2015**, *24*, 85–109. [CrossRef]
13. Horváth, B.; Szalai, I. Nonlinear Magnetic Properties of Magnetic Fluids for Automotive Applications. *Hung. J. Ind. Chem.* **2020**, *48*, 61–65. [CrossRef]
14. Chen, G.; Lou, Y.; Shang, T. Mathematic Modeling and Optimal Design of a Magneto-Rheological Clutch for the Compliant Actuator in Physical Robot Interactions. *IEEE Robot. Autom. Lett.* **2019**, *4*, 3625–3632. [CrossRef]
15. Standard Specification for Standard Nominal Diameters and Cross-Sectional Areas of AWG Sizes of Solid Round Wires Used as Electrical Conductors, ASTM International, 2014. Available online: <http://www.astm.org/Standards/B258.htm> (accessed on 1 August 2021).
16. Lord Corporation Product Bulletins. Available online: https://lordfulfillment.com/pdf/44/DS7012_MRF-140CGMRFluid.pdf (accessed on 1 August 2021).
17. Nguyen, Q.H.; Choi, S.B. Optimal design of an automotive magnetorheological brake considering geometric dimensions and zero-field friction heat. *Smart Mater. Struct.* **2010**, *19*, 11. [CrossRef]
18. Kluszczyński, K.; Pilch, Z. MR multi disc clutches—Construction, parameters and field model. In Proceedings of the 20th International Conference on Research and Education in Mechatronics (REM), Wels, Austria, 23–24 May 2019. [CrossRef]
19. Kluszczyński, K.; Pilch, Z. Basic features of MR clutches-resulting from different number of discs. In Proceedings of the 2019 15th Selected Issues of Electrical Engineering and Electronics (WZEE), Zakopane, Poland, 8–10 December 2019. [CrossRef]
20. Available online: <http://www.agros2d.org/> (accessed on August 2021).
21. Kowol, P.; Pilch, Z. Analysis of the magnetorheological clutch working at full slip state. *Electr. Rev.* **2015**, *91*, 108–111. [CrossRef]
22. Kluszczyński, K.; Pilch, Z. Integrated analytical-field design method of multi-disc magnetorheological clutches for automotive applications. *Bull. Pol. Acad. Sci. Tech. Sci.* **2021**, in print.
23. Pilch, Z. Analysis of Established Thermal Conditions for Magnetorheological Clutch for Different Loading Conditions. In *Analysis and Simulation of Electrical and Computer Systems*; Springer International Publishing: Berlin/Heidelberg, Germany, 2015; pp. 197–213. [CrossRef]